High-resolution Imaging System for Omnidirectional Illuminant Estimation

Shoji Tominaga, Tsuyoshi Fukuda**, and Akira Kimachi***
**Graduate School of Advanced Integration Science, Chiba University, Chiba 263-8522, Japan,*
***Department of Engineering Informatics, Osaka Electro-Communication University, Osaka 572-8530, Japan*

Abstract

The present paper realizes multiband spectral imaging with high spatial resolution for omnidirectional estimation of scene illuminant in a simple measuring system. To overcome the mirrored ball problems, we propose a multiband omnidirectional imaging system using a high-resolution trichromatic digital camera, a fisheye lens, and two color filters of commercial use. The spatial resolution of omnidirectional imaging systems is analyzed based on an optics model in detail. We describe a practical spectral imaging system. Use of the RGB camera with each of the two color filters allows two different sets of trichromatic spectral sensitivity functions via spectral multiplication, resulting in six spectral bands after two image captures with each color filter. An algorithm is developed on the statistical estimation theory for estimating illuminant spectra from noisy observations of the sensor outputs. The feasibility of the proposed method is examined from the viewpoints of spatial resolution and omnidirectional illuminant estimation.

Introduction

Most omnidirectional measuring system used a mirrored ball as an optical tool for capturing omnidirectional scenes [1][2]. A mirrored ball system is convenient to observe the surrounding scene of the ball placed at a particular point in space. In previous works, the authors first proposed a method for estimating an omnidirectional distribution of the scene illuminant spectral-power distribution from images taken by a camera aimed at a mirrored ball [3]. This imaging system had only RGB three channels of a digital color camera. Next an extended imaging system was developed for estimating precisely complicated spectral curves in natural scene illuminants [4]. The total system consisted of the mirrored ball and the multi-band imaging system using a monochrome digital camera and a liquid-crystal tunable filter (or color filters) in front of the camera.

This system, however, had several problems. The first is low and non-uniform spatial resolution, especially near the edge of the mirror. The second is a dead region due to imaging the camera itself reflected by the mirror. That is, there always is scene occlusion by the camera itself. The third is the indirect measurement of omnidirectional scene by using a mirrored ball. We have to calibrate the observed image data of the scene by using the surface-spectral reflectances on the mirror. In addition, even a small defect on the shape of the mirror can cause a significant image distortion, which will affect the accuracy in recovering panoramic images. Fourth, it takes much time for multi-spectral image acquisition in omnidirectional scene and high cost for narrowband filtration.

In this paper, our goal is to realize multiband spectral imaging with high spatial resolution for omnidirectional estimation of scene illuminant in a simple measuring system. To overcome the above problems, we propose a multi-band omnidirectional imaging system using a single-lens-reflex (SLR) RGB trichromatic digital camera, a fisheye lens, and two color filters of commercial use. It should be noted that a tunable filter (or color filter set) is unsuitable to place in front of the fisheye lens for multispectral imaging, because it limits the field of view by vignetting and the spectral imaging process becomes complicated due to significant dispersion by oblique light rays through the filter. To solve this problem, we adopt the combination of two color filters and a commercial high-resolution RGB camera, instead of a narrow band filter and a monochrome camera. Use of the RGB camera with each of the two color filters allows two different sets of trichromatic spectral sensitivity functions via spectral multiplication, resulting in six spectral bands after two image captures with each color filter. The total spectral sensitivity functions of the imaging system are kept constant for any direction of incident light since the spectral transmittances of color filters are free of dispersion. The color filters are placed between the fisheye lens and the camera body to prevent vignetting.

In the following, first we analyze the spatial resolution of omnidirectional imaging systems, based on an optics model in detail. Second, we describe a practical spectral imaging system. An algorithm is presented for reliable estimation of illuminant spectra using the present system. The feasibility of the proposed method is demonstrated in experiments on natural scenes

Spatial Resolution in Omnidirectional Imaging Systems

We analyze the spatial resolution of omnidirectional imaging system using a mirrored ball and a fisheye lens, by deriving a mathematical expression for a light ray that arrives at a certain image point on the focal plane.

Imaging system using a mirrored ball

First, let us consider a geometrical optics model of a system using a mirrored ball. Figure 1 shows a cross section of the system that includes the center points of the lens, O, and of the mirror, A. In this cross sectional plane, we choose the z axis to coincide with the optical axis and take the x axis through point O. Let a, ρ and f denote the radius of the mirror, the distance of OA, and the distance between the focal plane and the lens center, respectively. Consider a light ray that is included in the zx plane and arrives at an image point at distance r from the optical axis. We assume that this ray is reflected at point P on the mirror with coordinates (x_p, z_p) and with incidence angle γ. The slope angle of this ray with respect to the z axis is $\pi - \gamma - \beta$ and the specular

reflection angle is γ. Hence the equation for this ray is expressed as

$$x = (z - z_P)\tan(\pi - \gamma - \beta) + x_P, \quad (1)$$

where β is an angle between the normal at (x_P, z_P) and the z axis. The unknowns x_P, z_P and β are obtained by solving the equations

$$x_P = z_P \tan\alpha = (a - z_P)\tan\beta = \rho\cos\beta \quad (2)$$

where α is determined by $\alpha = \tan^{-1}(r/f)$. γ is also obtained as $\gamma = \alpha + \beta$.

For an image sensor with a uniform sampling grid, the spatial resolution of the mirrored ball system is graphically represented by use of Eq. (1) as shown in Figure 2. The dotted outer circle represents a sphere encircling the imaging system. A reflected ray (blue line) toward the image sensor corresponds to one of incident rays (red lines) from the outer circle to the mirrored ball. Note that the rays sampled in equal intervals on the sensor come from the locations sampled in different intervals on the outer circle.

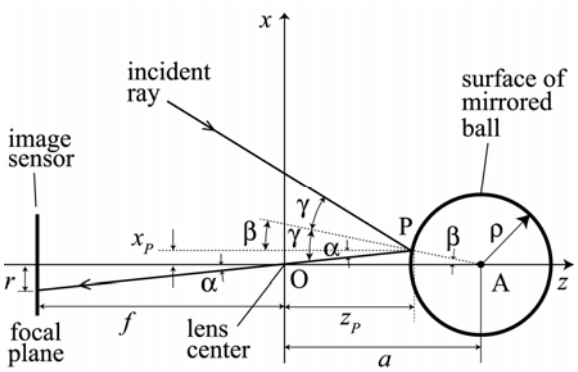

Figure 1 Geometrical optics model of a mirrored ball system.

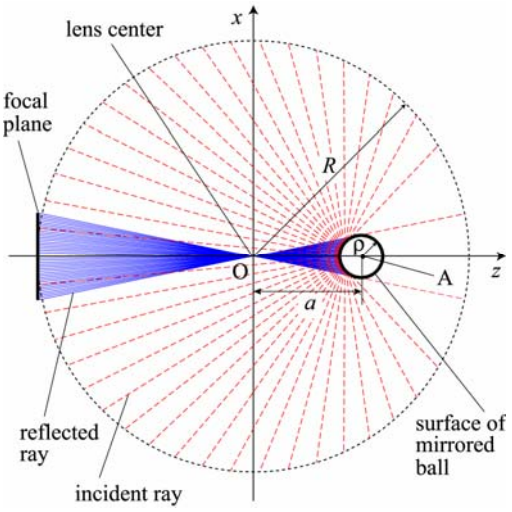

Figure 2 Spatial resolution map of an omnidirectional imaging system using a mirrored ball.

Imaging system using a fisheye lens

Next, we discuss an omnidirectional imaging system using a fisheye lens as depicted in Figure 3, where point O is the center of convergence of incident light rays and the z axis is the optical axis. There are two kinds of image projection methods. One is called equidistance projection, which is employed in a majority of fisheye lenses called $f\theta$ lenses. In equidistance projection, the light ray that arrives at an image point at distance r from the optical axis travels in the air before reaching the lens with an angle proportional to r, $\theta = r/f'$, with respect to the optical axis, where f' is the focal length of the lens. This characteristic directly allows a spatial resolution map as shown in Figure 4 for the same image sensor in Figure 2.

The other kind of projection is called orthographic or equi-solid-angle projection, in which the relation between θ and r is expressed as $\theta = \sin^{-1}(r/f')$. This projection yields a spatial resolution map shown in Figure 5

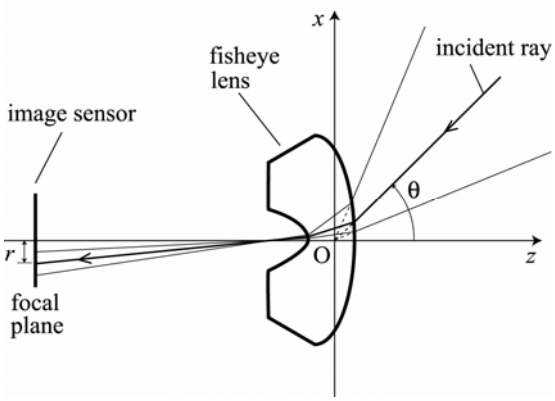

Figure 3 Geometrical optics model of a fisheye lens system.

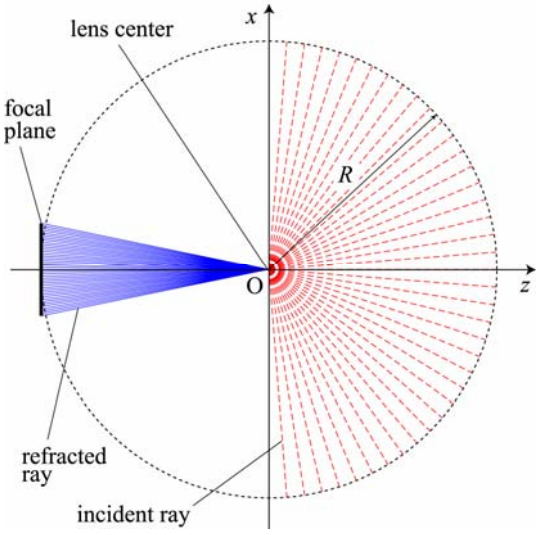

Figure 4 Spatial resolution map using an equidistance projection fisheye lens.

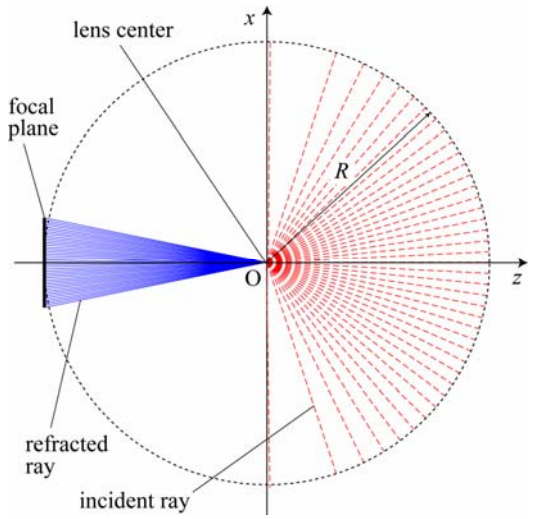

Figure 5 Spatial resolution map using an orthographic projection fisheye lens

Comparison in spatial resolution

Comparing Figures 2, 4 and 5, we note the fisheye lens systems achieve uniform spatial resolution, especially for equidistance projection, whereas the spatial resolution of the mirrored ball system is fine in the central part of the image sensor, but then becomes extremely coarse in the outer part near the optical axis. Moreover, the fisheye lens system allow finer spatial resolution than the mirrored ball system, especially in frontal directions for orthographic projection, although the mirrored ball system can cover a wider imaging area of over 180°.

For numerical evaluation, we computed the angular resolution and range of the mirrored ball system. We assumed a mirrored ball of 50-mm diameter, used in our previous studies [3] and a 1024x1024-pixel image sensor that barely covers the whole mirror region and is placed 500 mm away from it. Table 1 shows the results. In comparison, we computed the resolution as well for the two different fisheye lens systems with the same image sensor. The results confirm much better spatial resolution of fisheye lens systems than the mirrored ball system, even in the central part of the image sensor.

Table 1: Numerical comparison in angular resolution and range of mirrored ball and fisheye lens imaging systems. (ED: equidistance projection, OG: orthographic projection.)

	Angular range		Angular resolution	
	Min.	Max.	Min.	Max.
Mirrored ball	2.87°	357.13°	0.22°	7.15°
Fisheye lens (ED)	–90.00°	90.00°	0.18°	0.18°
Fisheye lens (OG)	–90.00°	90.00°	0.11°	3.58°

Multi-band Omnidirectional Imaging System

Figure 6 shows a system for multi-band omnidirectional imaging which is realized with a trichromatic digital camera, a fisheye lens, and a rotating table. The camera is a Canon EOS 1DS CMOS camera with the image size of 2718x4082 pixels and the bit depth of 12 bits. The camera response is linear in the level of raw data. The fisheye lens is a SIGMA Circular Fisheye lens based on the orthographic projection. The rotating table makes rotation in the horizontal plane. The rotation axis passes through the tip of the fisheye lens.

For multi-spectral image acquisition, we selected additional color filters from a set of commercial color filters. Figure 7 shows the spectral transmittance curves of these filters. Combining these transmittances to the original spectral sensitivities leads to different sets of trichromatic spectral sensitivity functions. The filter SP-6 is effective for shifting the spectral sensitivities to the short wavelength and long wavelength in the visible range, while the filter SP-7 is effective for shifting the spectral sensitivities to the middle wavelength. Thus, two sets of the modified trichromatic spectral sensitivities result in an imaging system with six spectral bands in the visible wavelength region. Figure 8 shows the overall spectral-sensitivity functions of the present multi-spectral imaging system. Each filter is placed between the lens and the camera body.

In this study, we do not use the two sets of trichromatic sensors without filter and with one additional filter [5]. This is because the magnitude of the sensor response decreases with additional filtration and the wavelength sensitivity regions modified by the additional filter overlap those of the original sensor. It is essential that the wavelength bands in a multi-spectral imaging system are independent of each other.

High-dynamic range images of natural scenes are captured by the present system. We used a shutter to extend the dynamic range of the present 12-bit camera. Pictures of the same scene are taken in different exposure times of 1, 1/2, 1/4/, ..., 1/100, ..., 1/8000 (sec), and the multiple images are combined into a single image.

We note that the intensity of a captured image depends on the pixel position. Figure 9 illustrates how the image intensity varies as a function of pixel position. The intensity decreases as the position is distant from the center of the image plane toward the edge. An inverse function to this characteristic curve, therefore, is used for correcting the observed image intensity.

Since the present fisheye system takes pictures of a scene in a hemisphere, we need at least two sets of images in opposite viewing directions for completing an omnidirectional image. To eliminate a certain distortion at the edge of the image plane, we can combine three sets of images observed at rotation angle intervals of 120 degrees.

We create an omnidirectional image as a latitude/longitude image in a polar coordinate system. The geometric transformation of captured images is done in two steps. The original images are first transformed into images by the equidistance projection, and then transformed into the polar coordinates. The definition and computation of the polar coordinates are described in the previous paper [4].

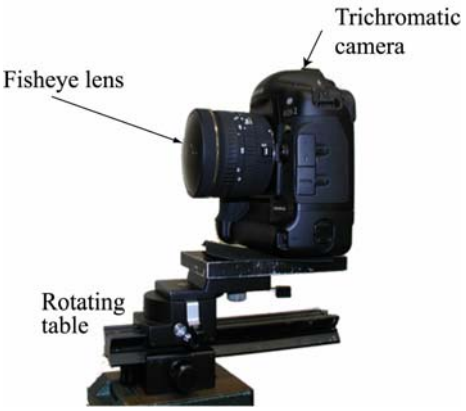

Figure 6 Omnidirectional imaging system.

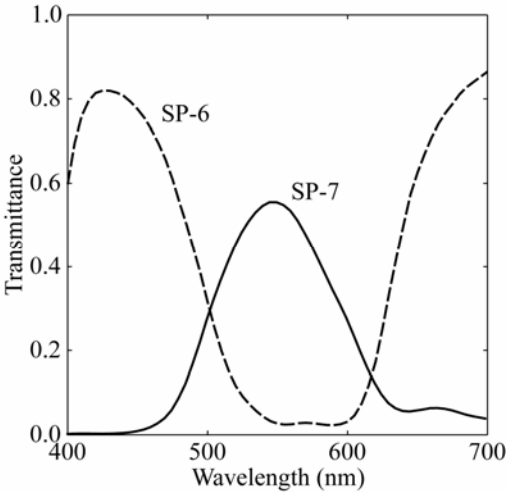

Figure 7 Additional color filters for multi-spectral imaging.

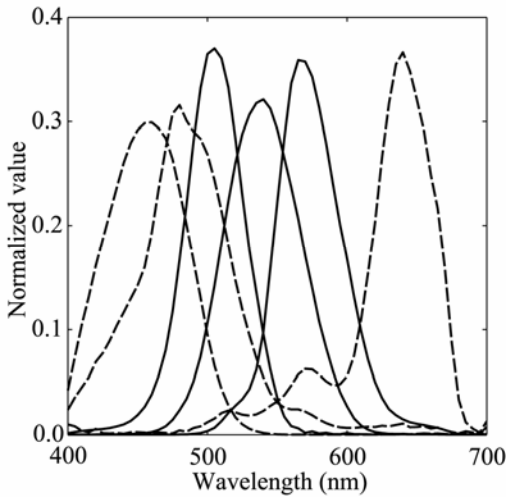

Figure 8 Overall spectral sensitivity functions.

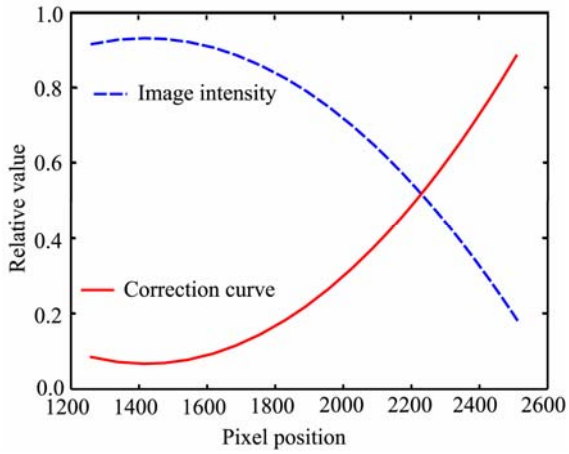

Figure 9 Variation of image intensity.

Estimation of Illuminant Spectra

Estimation algorithm

We have to recover the illuminant spectra in omni-directions from the noisy sensor outputs. Note that omnidirectional illuminants to be estimated are not only direct illuminations from light sources, but also indirect illuminations from light reflected from object surfaces in a scene. This study dones not use a finite-dimensional linear model for illuminant spectra. This approach is less reliable for noisy observations. The observed images can include various noise on sensors and optical process. Here we present an algorithm based on the statistical estimation theory.

The image sensor outputs are modeled as a linear system

$$\rho_i = \int_{400}^{700} E(\lambda) R_i(\lambda) d\lambda + n_i, \quad (i=1, 2, ..., 6) \qquad (3)$$

where $E(\lambda)$ is the illuminant spectrum, $R_i(\lambda)$ is the spectral sensitivity function of the i-th sensor, and n_i is the noise component with zero mean, including image sensor noise and an approximation error in the model. We sample each spectral function at n points with an equal interval $\Delta\lambda$ in the visible wavelength region [400, 700nm]. Let $\mathbf{e}$ be an n-dimensional column vector representing the illuminant spectrum $E(\lambda)$, $\overline{\mathbf{e}}$ be the mean illuminant vector, and $\mathbf{R}$ be a $6\times n$ matrix with the element $r_{ij} = R_i(\lambda_j)\Delta\lambda$. Moreover, define a six-dimensional column vector $\boldsymbol{\rho}$ representing a set of the sensor outputs ρ_i. Then the above imaging relationships are summarized in a linear matrix equation

$$\boldsymbol{\rho} = \mathbf{R}\,\mathbf{e} + \mathbf{n}. \qquad (4)$$

When the signal component $\mathbf{e}$ and the noise component $\mathbf{n}$ are uncorrelated, a linear minimum mean-squared error (LMMSE) estimate of $\mathbf{e}$ is given as

$$\hat{\mathbf{e}} = \overline{\mathbf{e}} + \mathbf{K}(\boldsymbol{\rho} - \mathbf{R}\overline{\mathbf{e}}), \qquad (5)$$

$$\mathbf{K} = \mathbf{C}_{ee}\mathbf{R}^t(\mathbf{R}\mathbf{C}_{ee}\mathbf{R}^t + \boldsymbol{\Sigma})^{-1} \qquad (6)$$

where $\mathbf{C}_{ee}$ is an $n \times n$ matrix of covariances between the elements of the illuminant vector and $\mathbf{\Sigma}$ is a 6×6 matrix of autocorrelations between sensor noises of each spectral channel. The covariance matrix of the estimation error is then given as

$$\mathbf{C}_{error} = \mathbf{C}_{ee} - \mathbf{K}\,\mathbf{R}\mathbf{C}_{ee} \quad . \tag{7}$$

To determine $\bar{\mathbf{e}}$ and $\mathbf{C}_{ee}$, we used a database of more than 500 surface-spectral reflectances for artificial objects and natural objects, and a set of 10 illuminant spectra, including an incandescent lamp and daylights. We created a large database of more than 5000 indirect illuminants by multiplying the surface-spectral reflectances and the illuminant spectra. The set of direct illuminants were added to the indirect illuminant database for completing the overall illuminant database.

Evaluation of sensor noise

It is important to obtain the noise covariance matrix $\mathbf{\Sigma}$ correctly for the reliable illuminant estimation. In this study, we present a simple approach of estimating $\mathbf{\Sigma}$ by directly evaluating the error in the sensor output domain. We use sample surfaces whose spectral reflectances are known. We can assume that the noises in each spectral channel are statistically independent. In this case, the covariance matrix is reduced to be diagonal as $\mathbf{\Sigma} = \mathrm{diag}(\sigma_1^2, \sigma_2^2, ..., \sigma_6^2)$.

We directly apply Eq. (4) for a set of samples surfaces for estimating $\mathbf{\Sigma}$, for which known surface-spectral reflectances and their sensor outputs are substituted for $\mathbf{e}$ and $\boldsymbol{\rho}$, respectively. First, we predict $\hat{\boldsymbol{\rho}} = \mathbf{R}\mathbf{e}$ by using the known surface-spectral reflectance of a sample surface and the known illuminant spectrum of a light source. Next, the predicted sensor output $\hat{\boldsymbol{\rho}}$ and the observed sensor output $\boldsymbol{\rho}$ are substituted for Eq. (4). The noise variance σ_i^2 in each channel is estimated as an average of the prediction errors $\boldsymbol{\rho} - \hat{\boldsymbol{\rho}}$ over all observations for the samples.

Experimental Results

To estimate the noise variance in our spectral imaging system, we have carried out an experiment using a Macbeth Color Checker and a test illuminant. The spectral reflectances of the color patches in the color checker and the spectral power distribution of the incandescent lamp were measured in advance. We have evaluated the signal-to-noise (S/N) ratio for each channel independently. This ratio depends on the magnitude of the sensor sensitivity function. The average S/N ratio was about 30 dB.

Second, we have examined the estimation accuracy of illuminant spectra. The Macbeth Color Checker was also used in this examination. That is, the reflected light from a color patch under a light source was used as a test illuminant. The images of the color checker were taken with the imaging system under two light sources. So we had two sets of illuminants, each of which consists of 24 colored lights corresponding to 24 color patches. Table 2 lists the statistical data on the estimation errors $\mathbf{E}[\| \mathbf{e} - \hat{\mathbf{e}} \|^2]$, which is defined as difference between the estimate and the measurement. The estimation accuracy by the proposed method using the multi-spectral imaging system is compared with the one by the trichromatic imaging system.

Third, we have examined the spatial resolution of the omnidirectional image captured with the proposed system. Image acquisition for this purpose was done in a class room. Figure 10 shows a part of the room that includes a curtain at a window. Let us notice the waves (folds) of the curtain. The proposed fisheye system presents a clear image of the waves of the curtain. On the other hand, the same scene was photographed using the mirrored ball system with the same camera as the fisheye system. In Figure 10(b), we cannot recognize the wave of the curtain at all. These comparisons suggest that the proposed system is superior to the previous system in the spatial resolution.

Finally, we have performed the omnidirectional imaging for outdoor scene. Figure 11 shows the omnidirectional image of a courtyard under daylight. We took several images of the same scene with different shutter speeds for acquiring a high dynamic range image. Then, three high dynamic range images in three viewing directions were combined. Finally, these images were transformed into polar coordinates. The image in Figure 11 is the resultant latitude/longitude image. This image clearly exhibits the details of the scene. Figure 12 shows the estimation results of illuminant estimation for Area 1- Area 4 in the scene. The comparisons between the estimates and the measurements suggest the reliability of the proposed estimation method based on multi-spectral imaging.

Table 2 Performance of illuminant estimation.

		Illuminant estimation error	
		Incandescent	Slide projector
Trichromatic imaging system	Average	0.00046474	0.00097966
	Max	0.00203628	0.00526681
Six-channel imaging system	Average	0.00008269	0.00037539
	Max	0.00026565	0.00080530

(a) (b)

Figure 10 Images with different spatial resolutions. (a) Proposed imaging system (b) Previous imaging system

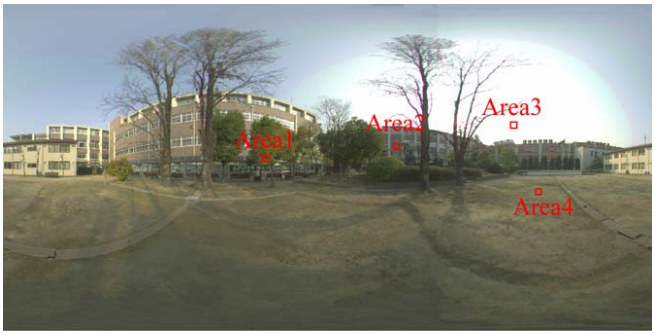

Figure 11 Omnidirectional image of an outdoor scene.

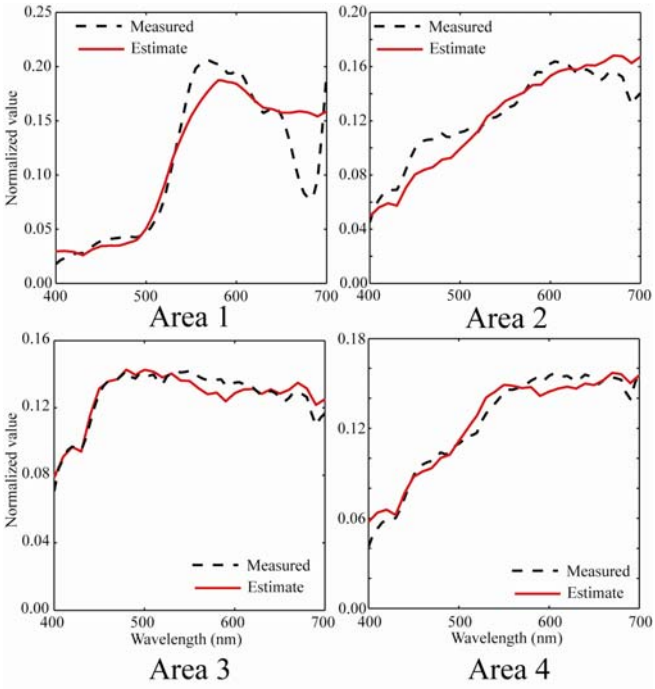

Figure 12 Estimation results of illuminant spectra.

Conclusion

This paper has described multiband spectral imaging with high spatial resolution for omnidirectional estimation of scene illuminant in a simple measuring system. A multiband omnidirectional imaging system was proposed using a high-resolution trichromatic digital camera, a fisheye lens, and two color filters. The spatial resolution of omnidirectional imaging systems was analyzed based on an optics model in detail. The present system overcomes the mirrored ball problems, such as the low and non-uniform spatial resolution and the dead region due to imaging the camera itself. Use of the RGB camera with each of the two color filters allowed two different sets of trichromatic spectral sensitivity functions via spectral multiplication, resulting in six spectral bands. An algorithm was developed on the statistical estimation theory for estimating illuminant spectra from noisy observations of the sensor outputs. The estimation accuracy was examined using Macbeth Color Checker and standard light sources. Finally, the feasibility of the proposed method was confirmed from the viewpoints of spatial resolution and omnidirectional illuminant estimation.

References

[1] P. E. Debevec, "Rendering synthetic objects into real scenes," *Proc. SIGGRAPH 98*, pp.189-198 (1998)

[2] S. Tominaga and N. Tanaka, "Measurement of omnidirectional light distribution by a mirrored ball," *Proc. The Ninth Color Imaging Conf.: Color Science, Systems, and Applications*, pp.22-26 (2001).

[3] S. Tominaga and N. Tanaka, "Feature Article: Omnidirectional scene illuminant estimation using a mirrored ball," *J. Imaging Science and Technology*, Vol.50, No.3, pp.217-227 (2006)

[4] S. Tominaga and T. Fukuda, "Omnidirectional scene illuminant estimation using a multispectral imaging system," *Proc, SPIE, Color Imaging XII*, Vol.6493 (2007)

[5] F.H. Imai and R.S. Berns, "Spectral estimation using trichromatic digital camera," *Proc. of International Symp. Multispectral Imaging and Color Reproduction for Digital Archives,* pp.42-49 (1999).

Author Biography

Shoji Tominaga received the B.E., M.S., and Ph.D. degrees in electrical engineering from Osaka University, in 1970, 1972, and 1975, respectively. From 1976 to 2006, he was at Osaka Electro-Communication University, Osaka. In 2006, he joined Chiba University, where he is currently a professor of Department of Information Science. His research interests include color image synthesis/analysis and multi-spectral imaging. He is President of the Color Science Association of Japan and a Fellow of IEEE and IS&T.